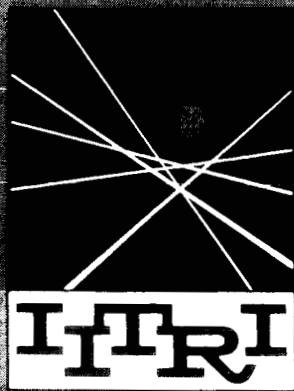


4/5p

N64-16757A



IIT RESEARCH INSTITUTE
formerly Armour Research Foundation of Illinois Institute of Technology

OTS PRICE

XEROX

MICROFILM

Technology Center

Chicago, Illinois 60616

UNPUBLISHED PRELIMINARY DATA

Report No. IITRI-C6018-6
(Quarterly Report)

INVESTIGATION OF LIGHT SCATTERING
IN HIGHLY REFLECTING PIGMENTED COATINGS

National Aeronautics
and Space Administration

IIT RESEARCH INSTITUTE

(NASA CR-53118; ?)

Report No. IITRI-C6018-6
(Quarterly Report)

INVESTIGATION OF LIGHT SCATTERING
IN HIGHLY REFLECTING PIGMENTED COATINGS

October 1, 1963 - to January 1, 1964

(NASA Contract No. NASr-65(07)
IITRI Project C6018)

OTS: \$4.60, \$1.55 ref

☒ OTS
☒ 2

Prepared by

G. A. Zerlaut, S. Katz, and J. Stockham

of

1182062

IIT RESEARCH INSTITUTE
Technology Center
Chicago 16, Illinois

for

National Aeronautics and Space Administration
Office of Advanced Research and Technology
Washington, D. C.

Copy No. 8

January 29, 1964

45p

FOREWORD

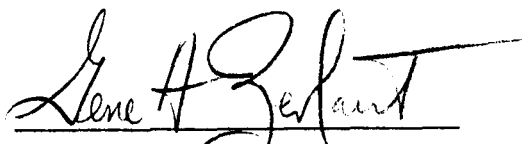
This is Report No. IITRI-C6018-6 (Quarterly Report) of Project C6018, Contract No. NASr-65(07), entitled "Investigation of Light Scattering in Highly Reflecting Pigmented Coatings." This report covers the period from October 1, 1963, to January 1, 1964.

Major contributors to the program include Gene A. Zerlaut (Project Leader), Dr. S. Katz (theoretical analyses), J. Stockham (principal investigator), V. Raziunas (light-scattering measurements), and Mrs. J. Allen (silver halide preparations). Contributions to this report were made by Dr. S. Katz, J. Stockham, and V. Razinuas.

Data are recorded in Logbooks C14085 and C13906.

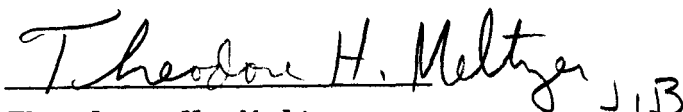
Respectfully submitted,

IIT RESEARCH INSTITUTE



Gene A. Zerlaut
Research Chemist
Polymer Research Section

Approved by:



Theodore H. Meltzer
Manager
Polymer Research Section

GAZ/jmh

ABSTRACT

16757^{over} INVESTIGATION OF LIGHT SCATTERING
IN HIGHLY REFLECTING PIGMENTED COATINGS 29

Investigations were conducted in the preparation of arrays of silver halide crystals in order to explain the scattering behavior of polydisperse pigmented coatings. The theory deals with arrays of uniform size and spacing, and a principal objective is the determination of how closely this idealized arrangement must be followed to achieve the desired results in practical formulations. These problems cannot be resolved satisfactorily by theory, and therefore an intensive experimental program is required.

The first portion of this report deals with the scattering of light by nontransparent spheres and is an extension of the general discussion of light scattering by particles which was begun in the first quarterly report. Both partially absorbing and totally reflecting spheres are discussed. The preparation of silver halide sols for the determination of optical properties is also discussed. The production of small crystals can be assured through decreasing the solubility of the crystals by the common ion effect, by removing all complexing agents, by producing the crystals at lower temperatures, and by adding the reagents rapidly to quickly attain and maintain a high degree of supersaturation. The production of large crystals can be maximized by increasing the solubility of the crystals with complexing agents, by use of high temperatures,

16757

by adding the reagents slowly, and by aging the crystals. In the ultraviolet, the reflectance of silver chloride coatings inverts with respect to concentration at approximately 2800 Å, and the maximum reflectance shifts toward larger wavelengths as the concentration increases. This is thought to be due to interaction of the particles; they effectively act as larger particles at the higher concentration. This inversion and shift have not been noted for larger particles. Angular light-scattering measurements were made on these films with the Brice-Phoenix light-scattering photometer. Comparison of the radial distribution of back-scattered light for various particle sizes with the theoretically predicted distribution gives a qualitative agreement.

AUTHOR

TABLE OF CONTENTS

	Page
Abstract	iii
I. Introduction	1
II. Concept of Light Scattering by Particles	2
A. Introduction	2
B. Light Scattering by Partially Absorbing Spheres	3
C. Light Scattering by Totally Reflecting Spheres	8
III. Experimental Work	10
A. Preparation of Sols	10
B. Preparation of Thin Films	22
IV. Measurement of Optical Properties	22
A. Reflectance and Transmittance Measurements	22
B. Angular Scattering of Light by Silver Chloride Films	27
C. Reflectance and Transmittance Measurements of Monodisperse Silver Chloride Films of Various Particle Sizes	32
V. Future Work	37

LIST OF TABLES AND FIGURES

		Page
Table		
1	Preparation of Silver Chloride Suspensions.	15
Figure		
1	Extinction, Absorption, and Scattering Coefficients (K_e , K_a , and K_x) for $m = 1.27-1.37$ i	7
2	Variation of Extinction Coefficient for a Spherical Particle as the Imaginary Part of the Refractive Index is Varied for $m = 1.29$ ($1 - i k$)	7
3	Radial Scattering Diagram for Very Small Totally Reflecting Spheres	9
4	Total Scattering Diagram for Totally Reflecting Spheres	9
5	Crystal Growth Apparatus	12
6	Electron Photomicrographs of Silver Chloride Crystals	16
7	Electron Photomicrographs of Silver Chloride Crystals	17
8	Electron Photomicrographs of Silver Chloride Crystals	18
9	Size Distribution of Silver Chloride Crystals (No Aging)	19
10	Size Distribution of Silver Chloride Crystals After 6 Hr of Aging	20
11	Effect of Aging on Silver Chloride Crystals	21
12	Transmittance of Coatings of Silver Chloride Suspensions in Gelatin at Various Concentrations	24
13	Absorbance of Coatings of Silver Chloride Suspensions in Gelatin	25

Figure		Page
14	Reflectance of Coatings of Silver Chloride Suspensions in Gelatin at Various Concentrations (Relative To MgCO_3)	26
15	Brice-Phoenix Light-Scattering Photometer	28
16	Intensity/Unit Area of Blue Mercury Line Versus Angle of Observation	29
17	Intensity/Unit Area of Green Mercury Line versus Angle of Observation	30
18	Intensity/Unit Area of Total Mercury Radiation versus Angle of Observation	31
19	Radial Distribution of Intensity of Back- Scattered Light for Various Particle Sizes	33
20	Reflectance of Silver Chloride Coatings of Various Particle Sizes and Concentrations	35
21	Transmittance of Silver Chloride Coatings of Various Particle Sizes and Concentrations	36

INVESTIGATION OF LIGHT SCATTERING IN HIGHLY REFLECTING PIGMENTED COATINGS

I. INTRODUCTION

The principal objective of this program is the application of single-particle scattering theory to particle arrays in an attempt to explain the scattering behavior of polydisperse pigmented coatings, especially highly reflecting pigmented coatings. In this respect, the program is aimed at a definition of the light-scattering parameters which are necessary for the maximum reflection of solar radiation. The definition and explanation of these factors should facilitate the eventual development of more highly efficient solar reflectors and, perhaps more important, should serve to extend our ability to apply light-scattering theory to the solution of other problems.

Because of the complex nature of the mathematics, the theory deals with particle arrays of uniform size and spacing. A principal question is: How closely must this idealized arrangement be followed to achieve the desired results in practical formulations? Furthermore, the optimum particle size is a function of wavelength, and therefore some optimum size distribution instead of a narrow size distribution is desirable. The chance of finding a pigment whose refractive index varies with the wavelength such that a single particle size will be optimum over a wide spectral range is remote. These questions and the related problem of pigment spacing

cannot be resolved satisfactorily by theory, and thus an intensive experimental program is required.

II. CONCEPT OF LIGHT SCATTERING BY PARTICLES

A. Introduction

This section continues the review of light-scattering theory begun in the first quarterly report. In that report the light-scattering properties of transparent spherical particles were considered, and both total and angular scattering intensity were described. In the present report the scattering of light by nontransparent spheres is discussed.

It was noted that the total scattering of light by spherical particles is a function of three parameters: the particle size, the refractive index of the particle in relation to the surrounding medium, and the wavelength of the light. For greatest generality, the refractive index is written as a complex number; the real part corresponds to the refractive index as it is usually written, and the imaginary part is related to the absorbing properties of the scatterer. The complex refractive index, n^* , is defined by

$$n^* = n (1 - i k) \quad (1)$$

Three special cases can be considered:

1. When $k = 0$, $n^* = n$, and the particle is transparent at that wavelength. (This case was discussed in Report No. IITRI-C6018-3.)

2. When k is a finite number, the particle both scatters and absorbs incident light. The absorption coefficient, μ , is related to k :

$$k = \frac{\lambda \mu}{4 \pi}$$

3. n^* can approach infinity by one of two routes:

$$n \longrightarrow \infty$$

or

$$k \longrightarrow \infty$$

The case of infinite refractive indices is examined in Section IIC.

B. Light Scattering by Partially Absorbing Spheres

The total scattering coefficient for a plane wave incident on a spherical particle is given by Mie as the sum of the convergent series.

$$K_c(a, n) = \frac{2}{\alpha^2} \sum_{m=1}^{\infty} (2m + 1) \left[|a_m|^2 + |b_m|^2 \right] \quad (2)$$

This is identical to Equation 4 of Report C6018-3 except for the use of subscripts with K to emphasize the distinction between transparent and partially absorbing spheres. The total Mie extinction coefficient is

$$K_e(\alpha, n) = \frac{2}{\alpha^2} \operatorname{Re} \sum_{m=1}^{\infty} (2m + 1) (a_m + b_m) \quad (3)$$

Only the real parts of the amplitude functions, a_m and b_m , contribute to the extinction.

The extinction defines the attenuation of the incident beam by all causes. In the present case, the extinction

includes both absorption and scattering, i.e.,

$$K_e = K_s + K_a$$

where K_a is the absorption coefficient. If the particle is a pure scatterer with no absorption, $K_e = K_s = K$, where K is the scattering coefficient of a transparent particle.

It is of interest to consider Equations 2 and 3 further. The influence of the complex term on the scattering properties of the particle is of importance. In addition, the physical significance of the complex number requires some examination. There are a number of compilations of the scattering of light by complex scatterers, and a few publications describe the effect of progressive change in the complex term of the scattering cross section. Some numerical magnitudes of the complex term for several materials will be discussed first.

A moderately absorbing material, such as a tinted glass, has a very small imaginary term. A fairly dense black glass, which transmits only 8% of the incident intensity through 1-mm thickness, has a refractive index of $1.5-0.001 i$. Actually this absorption is so slight for particles in the micron size range that the absorption can be neglected. Metals at optical frequencies have refractive indices whose coefficients are both near unity. Thus, the refractive index of iron at $\lambda = 0.44 \mu$ in the visible region is $1.27-1.37 i$. At longer wavelengths the refractive index terms of metals become very large and almost equal. At 10μ in the infrared,

the refractive index of platinum is 37-41 i. This is almost a totally reflecting material. Penndorf has compiled a bibliography of numerical computations on the scattering and absorption of electromagnetic radiation for spherical particles.¹

The complex attenuation by water in the infrared was studied by Johnson and his associates² and by Stephens,³ among others. Stephens has examined the total attenuation, the scattering, and the absorption cross sections of particles of diameters between 1.0 and 10 μ in the wavelength range between 4 and 90 μ .

There are very few compilations of radial scattering data for substances with complex refractive indices. A paper by Kerker⁴ describes the total and radial scattering of light by mercury droplets whose refractive index at 0.546 μ is 1.46-4.30 i.

¹Penndorf. "Research on Aerosol Scattering in the Infrared," Final Report, Air Force Cambridge Research Laboratories, Technical Report RAD-TR-63-26 (Report AFCRL-63-668), 1963.

²Johnson, Eldrige, and Terrell. Science Report No. 4, MIT Department of Meteorology, 1954.

³Stephens. "Total Attenuation, Scattering and Absorption Cross Sections of Water Droplets," Report AFCRL 1011, 1961.

⁴Kerker. "The Size and Shape of Colloidal Particles by Light Scattering," Technical Report No. 1, Clarkson College of Technology, ASTIA Report 26048, 1953.

In Figure 1, plots of the scattering, absorption, and total extinction cross sections for iron particles at 0.44μ are shown. It was noted that the complex refractive index of iron at this wavelength is $1.27-1.37 i$. This plot is of interest since it shows the relative contributions of scattering and absorption to the total attenuation. It is noted that at small values of α , the absorption is the principal contributor to the total attenuation. At $\alpha = 2$, the attenuations due to absorption and scattering are about equal, and beyond that, scattering predominates. Since $\alpha = 2 \pi r / \lambda$, scattering predominates at a wavelength of about 0.5μ for particles greater than $0.3\text{-}\mu$ diameter.

The effect of the gradual variation of the imaginary part of the complex refractive index on the total extinction coefficient has been computed by Johnson, Eldrige, and Terrell.² Figure 2 shows a portion of their calculations at low values of α for a series of refractive indices of the form $1.29 (1 - i k)$ as k varies from 0 to ∞ . The progressive changes in the extinction coefficient, K_e , with the changes in the imaginary part of the refractive index are clearly illustrated. In their extended analysis, Johnson, Eldrige, and Terrell noted that when the imaginary coefficient, k , is less than 0.10, the extinction curve oscillates as α increases. This recalls the scattering coefficient for nonabsorbing particles (Report C6018-3, Figure 1) which is the limiting case as $k \rightarrow 0$. At higher values of k , the oscillations after the first maximum disappear and the extinction

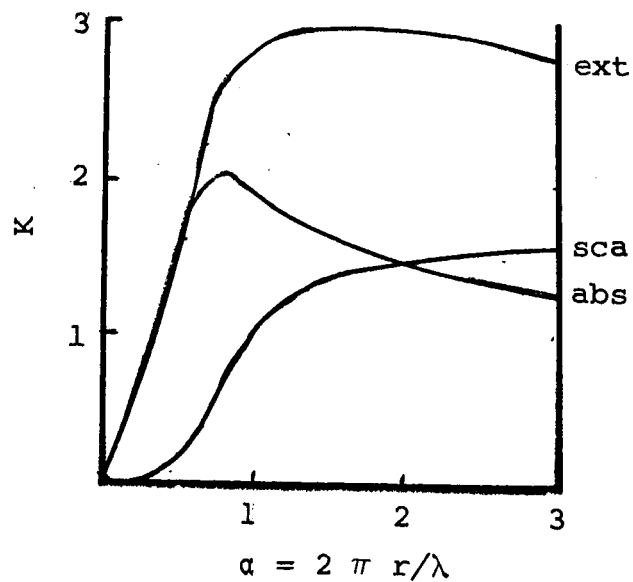


Figure 1
EXTINCTION, ABSORPTION, AND SCATTERING COEFFICIENTS
(K_e , K_a , and K_x) FOR $m = 1.27 - 1.37 i$

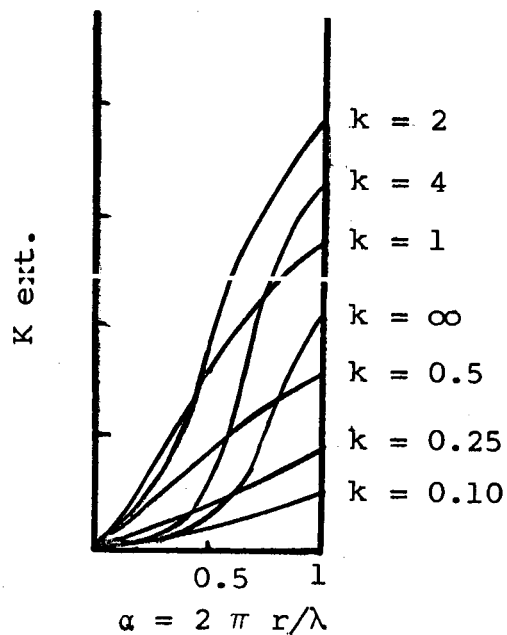


Figure 2
VARIATION OF EXTINCTION COEFFICIENT FOR A SPHERICAL PARTICLE
AS THE IMAGINARY PART OF THE REFRACTIVE INDEX IS VARIED
FOR $m = 1.29 (1 - i k)$

coefficient converges smoothly to the asymptotic value.

Kerker's data⁴ give the radial scattering intensities between 30 and 150°. Aden⁵ has analyzed the back-scattering of electromagnetic waves from spheres with complex refractive indices. Aden's procedure, which is especially adaptable to materials with complex refractive indices, includes a comparison of theoretical scattering in the region $0.74 \geq \alpha \geq 5.90$ and experimental data obtained on water droplets at microwave frequencies.

C. Light Scattering by Totally Reflecting Spheres

The case of spheres whose refractive index, m , equals infinity has been studied thoroughly because of its relative simplicity compared to the cases considered previously. The physical meaning of an infinite refractive index is that there is no penetration of the medium by the light. The problem can be considered as the limiting value either as the real or as the imaginary part of the refractive index increases to infinity; the results are the same in both cases.

Since a total reflector implies no penetration of the particle by incident radiation, Rayleigh scattering does not apply for even the smallest particles. The radial scatter for very small particles is shown in Figure 3. It is noted that the back-scattered intensity predominates over the forward

⁵Aden, J. Appl. Phys. 22, 601, 1951.

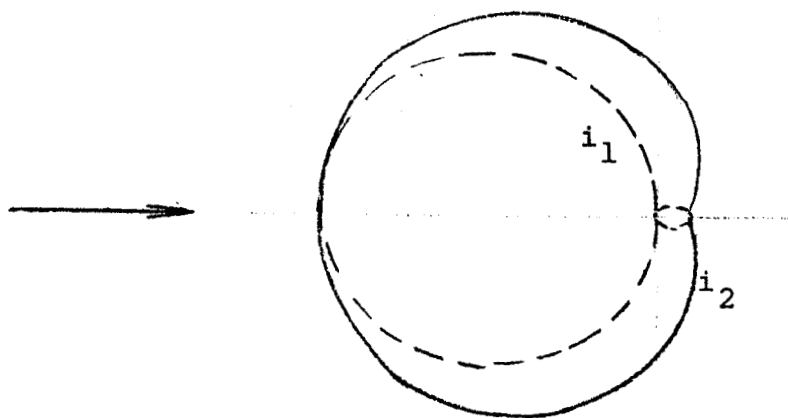


Figure 3

RADIAL SCATTERING DIAGRAM
FOR VERY SMALL TOTALLY REFLECTING SPHERES

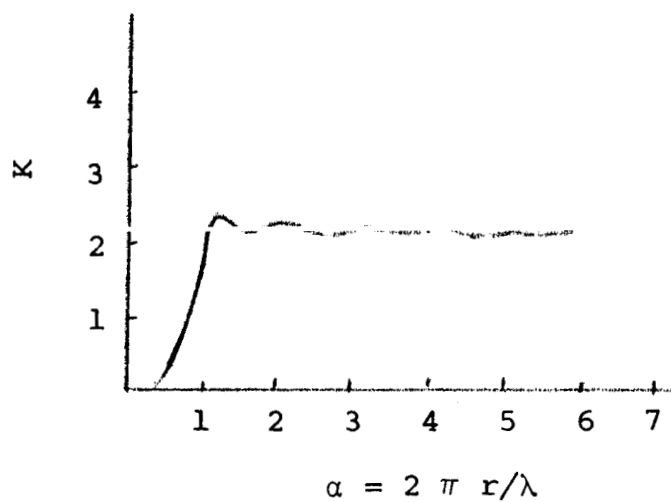


Figure 4

TOTAL SCATTERING DIAGRAM
FOR TOTALLY REFLECTING SPHERES

scatter by a factor of 9/1.* Radial scattering data for total reflectors for values of α between 0.5 and 10 are given by van de Hulst.⁶ At larger values of α , above about 1.4, the usual predominance of forward scatter over back scatter is noted. The total scatter of light by particles with infinite refractive index is shown in Figure 4. It is seen that the scattering, or extinction coefficient, which is the same in the absence of absorption, reaches a maximum slightly greater than the asymptotic value.

III. EXPERIMENTAL WORK

A. Preparation of Sols

Suspensions of silver halide crystals are being used to study the dependence of light scattering on the size and concentration of particles. The halide crystals are precipitated by the simultaneous addition at equal rates of equivalent solutions of silver nitrate and a potassium halide to a warm gelatin suspension, which serves to retard the coalescence of the crystals. The preparations are made in a darkroom under a red safety light. The photographic-grade gelatin was supplied by the Atlantic Gelatin Company. The apparatus for

⁶Van de Hulst. "Light Scattering by Small Particles," John Wiley and Sons, New York, p. 163, 1957.

*One characteristic of true Rayleigh scattering is the equal intensity of the forward- and back-scattered radiation.

the preparations is shown in Figure 5. Warm water from a constant-temperature bath is circulated between the walls of a double-walled vessel containing 100 ml of gelatin suspension. The gelatin is stirred magnetically during the addition of the chemical. A total of 30 ml of each reagent is added to the gelatin from 50-ml syringes; the feed rate is controlled by a Harvard infusion-withdrawal pump adapted to operate both syringes simultaneously. The effect of the following variables on crystal growth was studied: concentration of reactants, concentration of gelatin, reactant addition rate, temperature, growth modifiers, aging, addition of excess chloride, and storage stability.

The chemical addition rates are sufficient to quickly reach and maintain a high degree of supersaturation; thus, crystal growth does not depend on the presence of imperfections. In other words, the low solubility of the halides coupled with the rapid addition allows crystallization to proceed from a large number of centers of nuclei. When these primary particles are about the same sizes and have the same solubilities, there is little tendency for the larger particles to grow at the expense of the smaller ones.

If the precipitate is formed under conditions in which it is somewhat soluble or if the primary crystals have a solubility that is much greater than larger crystals, crystallization tends to start from fewer nuclei and larger crystals

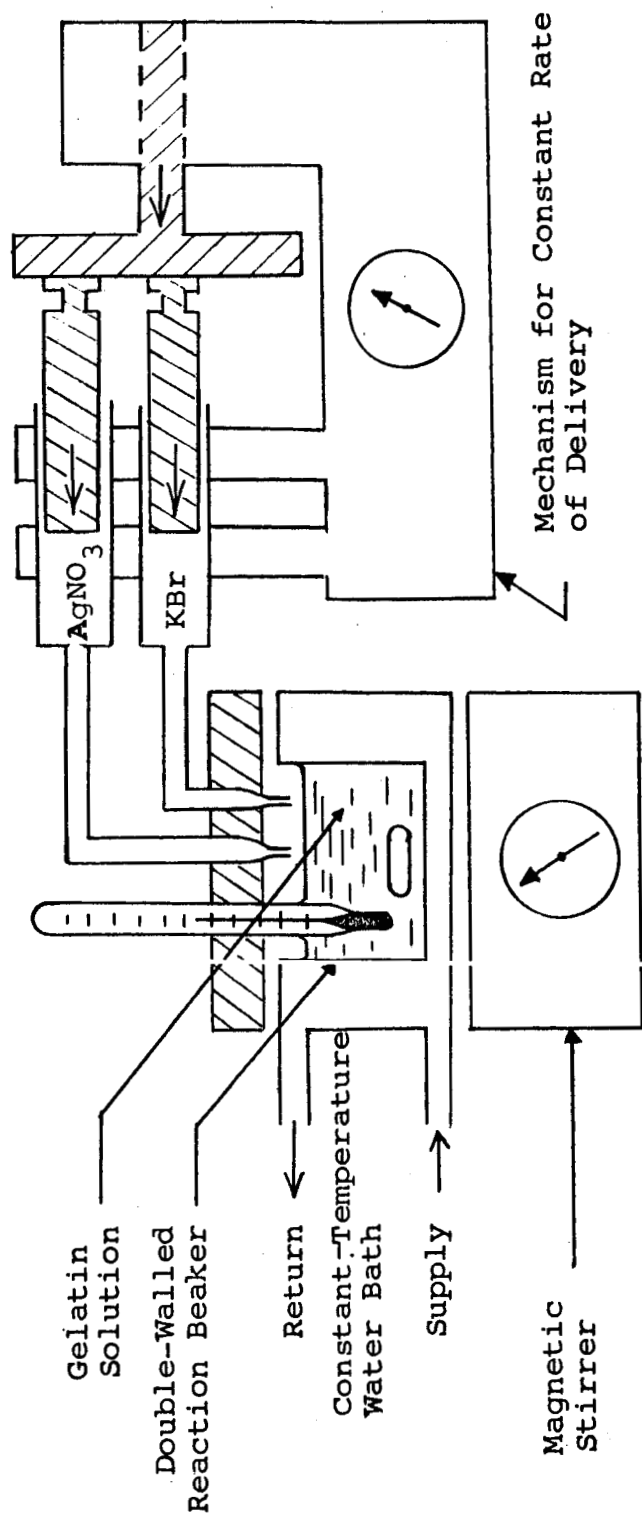


Figure 5
CRYSTAL GROWTH APPARATUS

tend to grow. Berry⁷ noted this effect in the addition of ammonia and other similar growth modifiers. In this regard, the solubility product of silver bromide at 25°C is 7.7×10^{-13} g-moles/liter and for silver chloride 1.6×10^{-10} g-moles/liter. Thus the use of ammonia with silver chloride might not have the same effect on crystal size as it does with silver bromide. With some crystalline substances, aging at elevated temperatures causes the smaller particles to dissolve slowly and recrystallize on the larger ones. The greater solubility of the smaller crystals is attributed to the existence of more isolated atoms or groups of molecules which can more readily break away from the crystal.

The production of small crystals can be maximized by decreasing the solubility of the crystals by the common ion effect, removing all complexing agents, producing the crystals at a lower temperature, adding the reagents rapidly to quickly attain and maintain a high degree of supersaturation, and not aging the crystals. The production of large crystals can be maximized by increasing the solubility of the crystals through the addition of complexing agents, producing the crystals at elevated temperature, adding the reagents slowly, and aging the crystals.

⁷Berry J. Opt. Soc. Am. 52, 588, 1962.

A summary of the crystals prepared to date is contained in Table 1. Figures 6, 7, and 8 are electron photomicrographs of typical particles. Batch 15 is of special interest. It was prepared by the relatively rapid addition of 3 N solutions of silver nitrate and potassium chloride to 100 ml of a 30-g/liter gelatin suspension maintained at 50°C. Immediately after the chemical addition, a 20-ml aliquot was diluted with 40 ml of gelatin. This aliquot was sampled immediately and after 24 hours of storage in a refrigerator. The particle size distributions are shown in Figure 9. The size distributions obtained for batches 2 and 8, reported previously, are also shown for comparison.

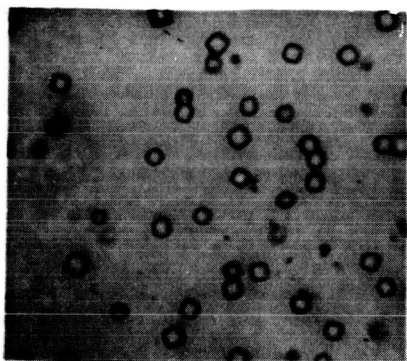
After 6 hours of aging at 50°C with continuous stirring, a second aliquot was removed and diluted with 40 ml of water. This aliquot was sampled immediately, after 1 day, and after 4 days of storage in the refrigerator. The size distribution analysis of these samples is shown in Figure 10.

After aging at 50°C for 24 hours, a third aliquot was removed and diluted with 40 ml of gelatin. This aliquot was sampled immediately, and its size distribution is shown in Figure 11. The distributions for the aliquot taken at the 0- and 6-hour aging periods are also shown.

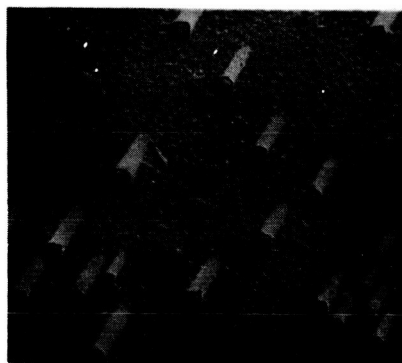
The results indicate that, in order to prevent the growth of abnormally large particles, the aging process at elevated temperature (50°C) should be stopped before 24 hours. The effect of prolonged storage under refrigeration is not clear.

Table 1
PREPARATION OF SILVER CHLORIDE SUSPENSIONS

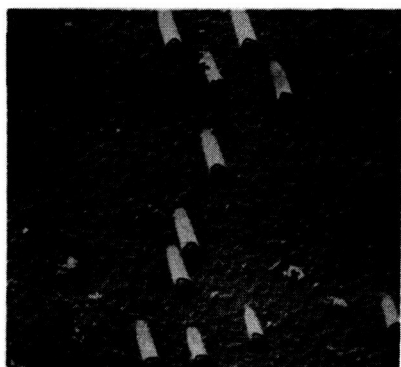
Batch No.	KCl and AgNO ₃ Normality	Addition Rate, ml/min	Reaction Temp., °C	Reaction pH	Gelatin Conc., g/liter	Excess KCl Added, ml	Aging Period hr	Notes
1	2	2	5.0	6.0	30	0	0	
2	2	2	5.0	6.0	30	2	0	Excess KCl added before ppt.
3	2	2	5.0	6.0	15	2	0	Excess KCl added before ppt.
4	2	2	6.1	9.0 (NH ₃)	30	2	0	Excess KCl added before ppt.
5	2	2	6.1	10.5 (NH ₃)	30	2	0	Excess KCl added before ppt.
6	2	2	6.1	9.0 (NH ₃)	5	2	0	Excess KCl added before ppt.
7	2	2	6.1	9.0 (NH ₃)	5	2	0	40 ml of 30-g/liter gelatin added after ppt., KCl added after ppt.
8	3	2	5.6	6.0	30	2	0	Excess KCl added after ppt.
9	3	2	5.0	6.0	30	2	0	Excess KCl added after ppt.
10	2	2	5.0	9.5 (NH ₃)	30	2	0	Solution divided, 2 ml added to one.
11	2	2	4.9	9.5 (NH ₃)	30	2	16	Excess KCl added after 16 hr.
12	3	15	5.0	6.0	30	2	0	Excess KCl added before ppt.
13	3	15	5.5	6.0	0	0	0	20 ml of 30-g/liter gelatin added after ppt.
14	0.2	0.4	5.0	6.0	5	0	0	
15	3	15	5.0	6.0	30	0	See text	



Batch 1
(10,500x)



Batch 2
(10,000x)



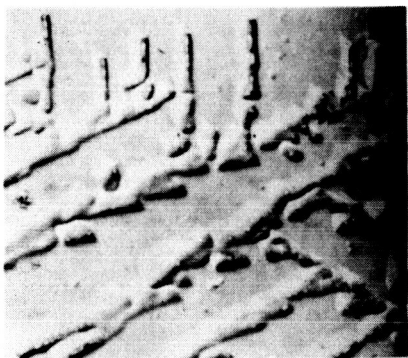
Batch 3
(10,500x)



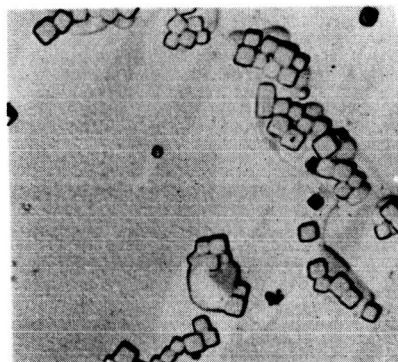
Batch 4
(10,000x)

Figure 6

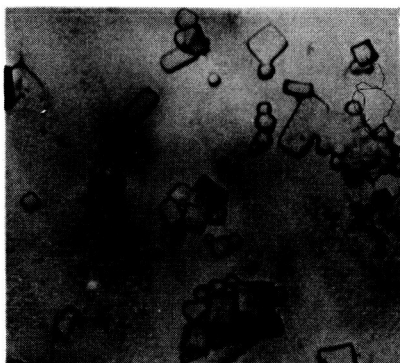
ELECTRON PHOTOMICROGRAPHS OF SILVER CHLORIDE CRYSTALS



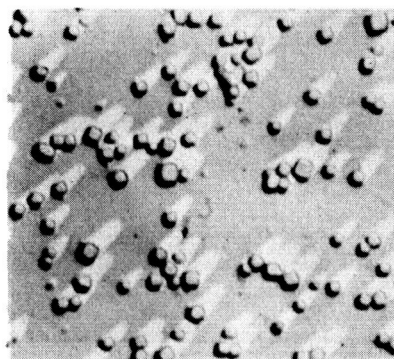
Batch 5
(5000x)



Batch 6
(10,000x)



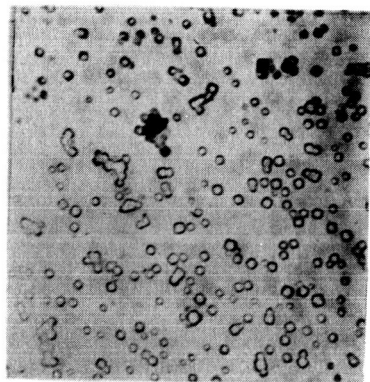
Batch 7
(10,000x)



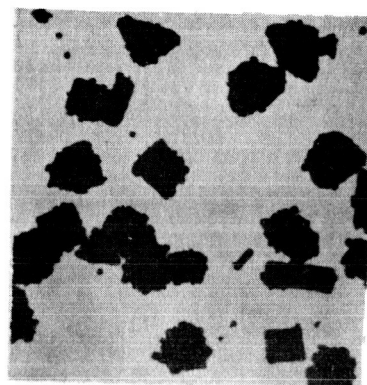
Batch 8
(10,000x)

Figure 7

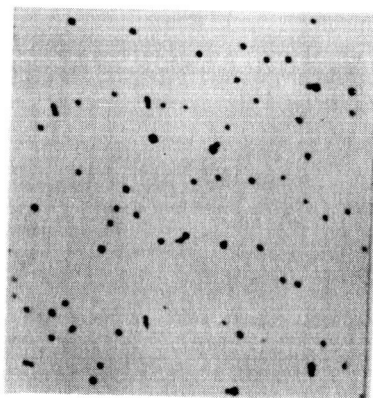
ELECTRON PHOTOMICROGRAPHS OF SILVER CHLORIDE CRYSTALS



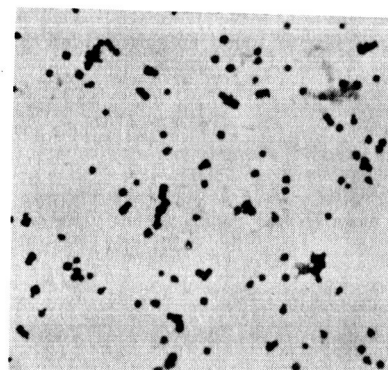
Batch 12
Immediately after
Preparation
(10,000x)



Batch 12
One Week
after Preparation
(5,000x)



Batch 14
Five days
after Preparation
(5,000x)



Batch 14
Ten days
after Preparation
(5,000x)

Figure 8

ELECTRON PHOTOMICROGRAPHS OF SILVER CHLORIDE CRYSTALS

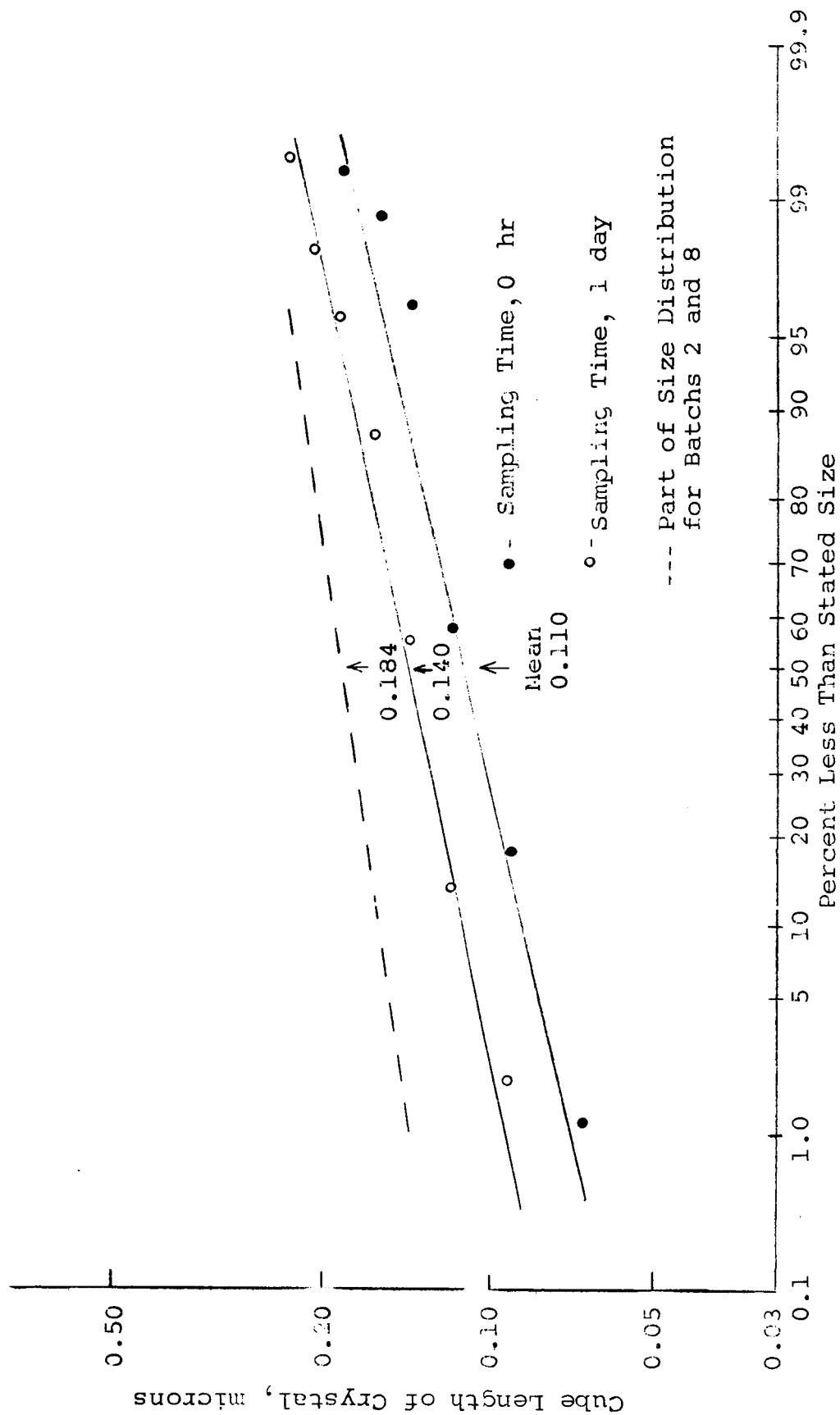


Figure 9

SIZE DISTRIBUTION OF SILVER CHLORIDE CRYSTALS (NO AGING)

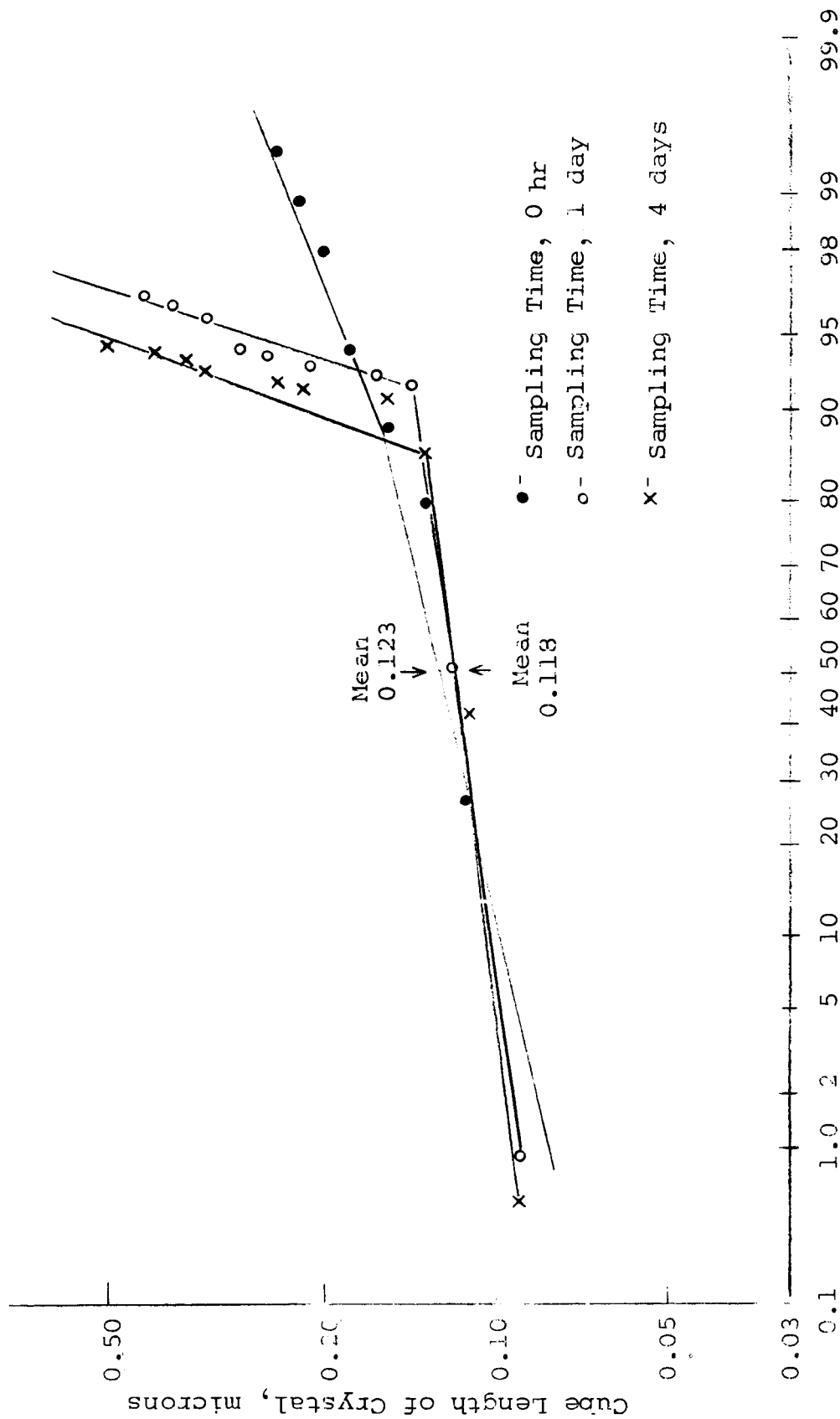


Figure 10

SIZE DISTRIBUTION OF SILVER CHLORIDE CRYSTALS
AFTER 6 HR OF AGING

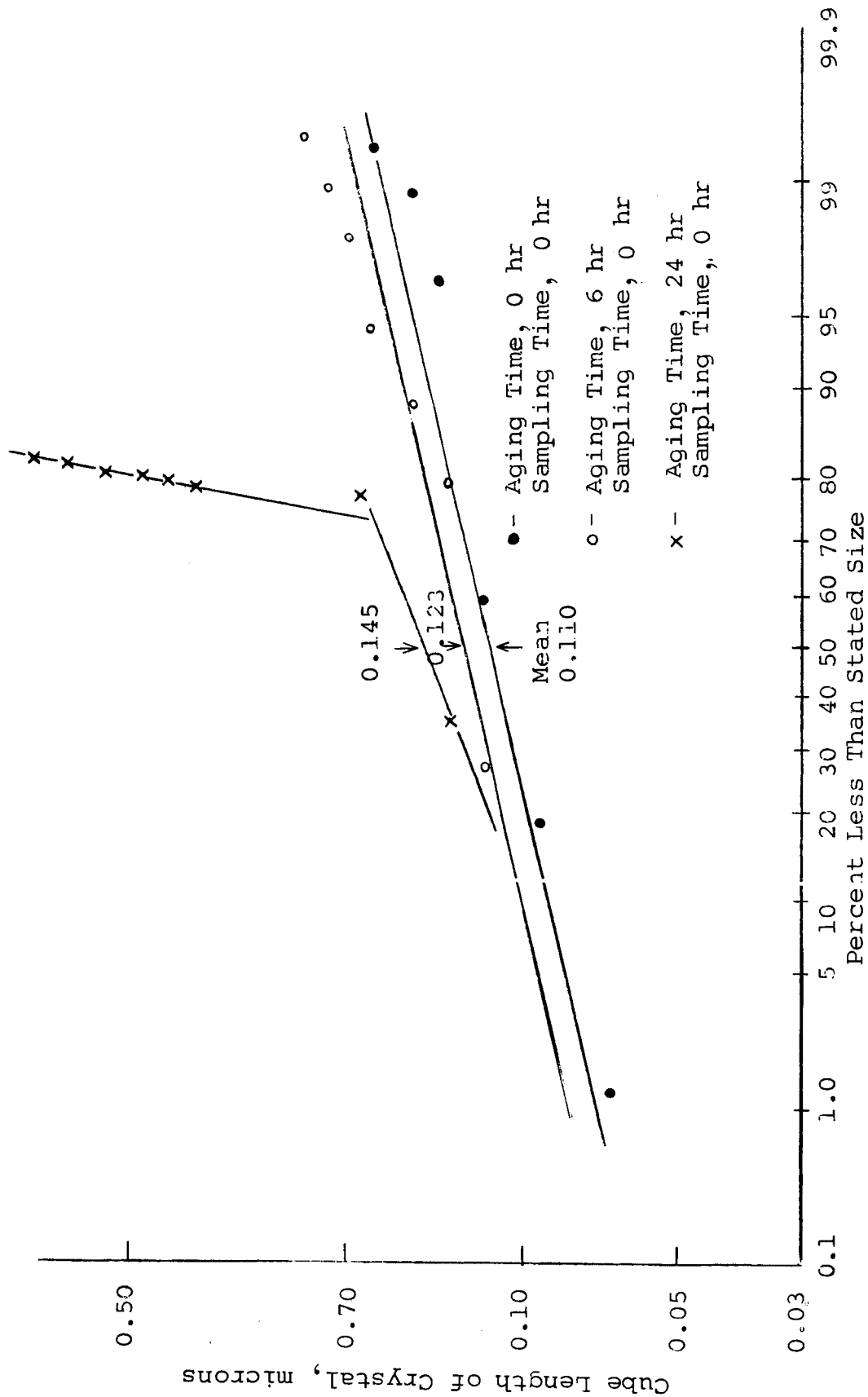


Figure 11

EFFECT OF AGING ON SILVER CHLORIDE CRYSTALS

Abnormally large particles were present after a 1-day storage for the 6-hour aged sample but were not present in the unaged sample similarly stored. However, the 6-hour aged sample was diluted with water and the gelatin concentration was so low that it did not "set" on refrigeration. This would permit greater mobility among the particles.

It appears that the best controls of particle size are addition rate and chemical concentration. Because the size distributions are log-normal with a low size variation just after preparation, the films used for spectrographic analysis should be prepared and examined immediately.

B. Preparation of Thin Films

Thin films are prepared for spectrographic study by spreading the fluid gelatin and crystal suspensions on quartz plates with a Gardner knife and quickly drying the suspensions in a stream of hot air. A film of uniform particle density and thickness is obtained once the skill of the operator is developed.

IV. MEASUREMENT OF OPTICAL PROPERTIES

A. Reflectance and Transmittance Measurements

Reflectance and transmittance spectra were measured with the Cary spectrophotometer. Transmission measurements were made using monochromatic incident light with a quartz plate coated with gelatin in the reference beam. Only parallel

transmission was monitored. Reflectance measurements were made using monochromatic incident light; the reflected light entered the integrating sphere and was received by the phototube. A light trap was placed behind the specimen in the reflectance measurements. In this manner, the bulk of the light stability problem experienced with silver halide arrays was circumvented.

The silver chloride coatings showed a transmission peak at 2400 Å and a minimum at about 2800 Å (Figure 12). These peaks are probably due to the crystal array since a uniform silver chloride window would be expected to give a monotonic, uniform decrease in transmission as the wavelength of light decreases. Figure 13 is a plot of the absorbance at several wavelengths and includes the transmittance and absorption peaks for the four concentrations of silver chloride coatings. If Beer's law is obeyed, a straight line would be obtained.

The reflectance of the coatings is plotted in Figure 14. The reflectance inverted with respect to the concentration in the ultraviolet region at approximately 2800 Å, and the maximum reflectance shifted toward larger wavelengths as the concentration increased. It is postulated that this is due to interaction of the particles in the more concentrated coatings; they are effectively acting as larger particles. The light stability of the coatings was not a problem during these measurements.

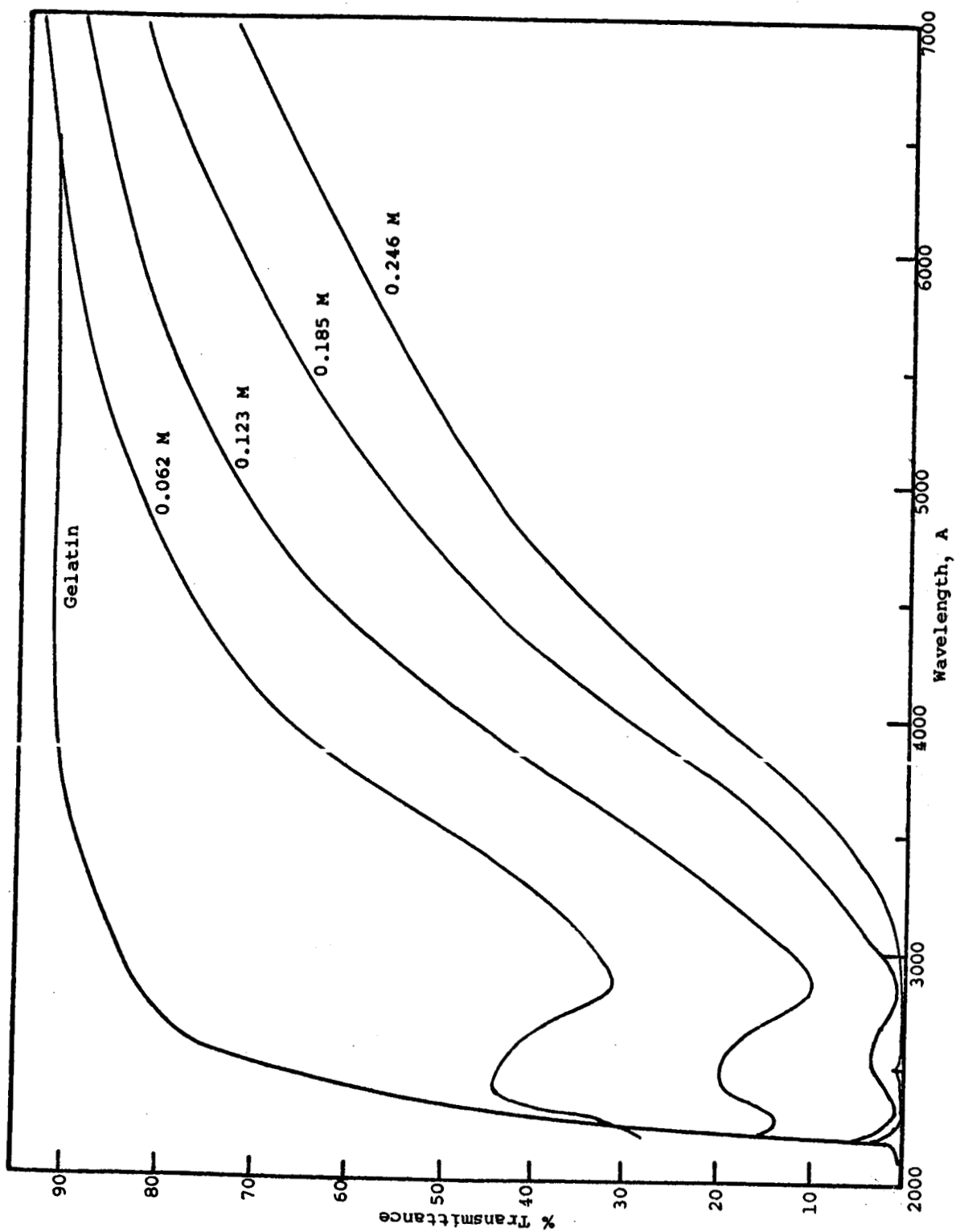


Figure 12
TRANSMITTANCE OF COATINGS OF SILVER CHLORIDE SUSPENSIONS
IN GELATIN AT VARIOUS CONCENTRATIONS

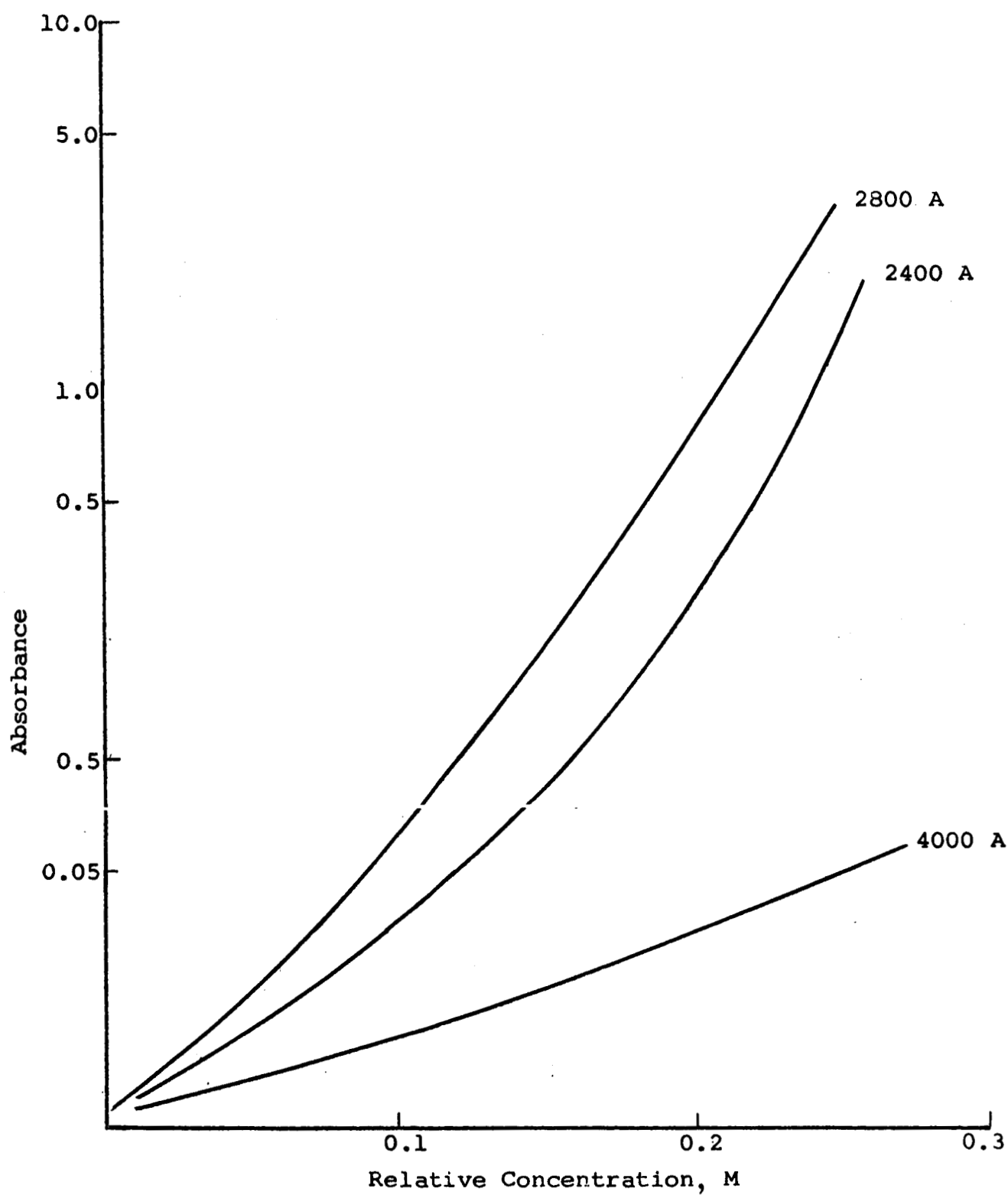


Figure 13

ABSORBANCE OF COATINGS OF SILVER CHLORIDE SUSPENSIONS
IN GELATIN

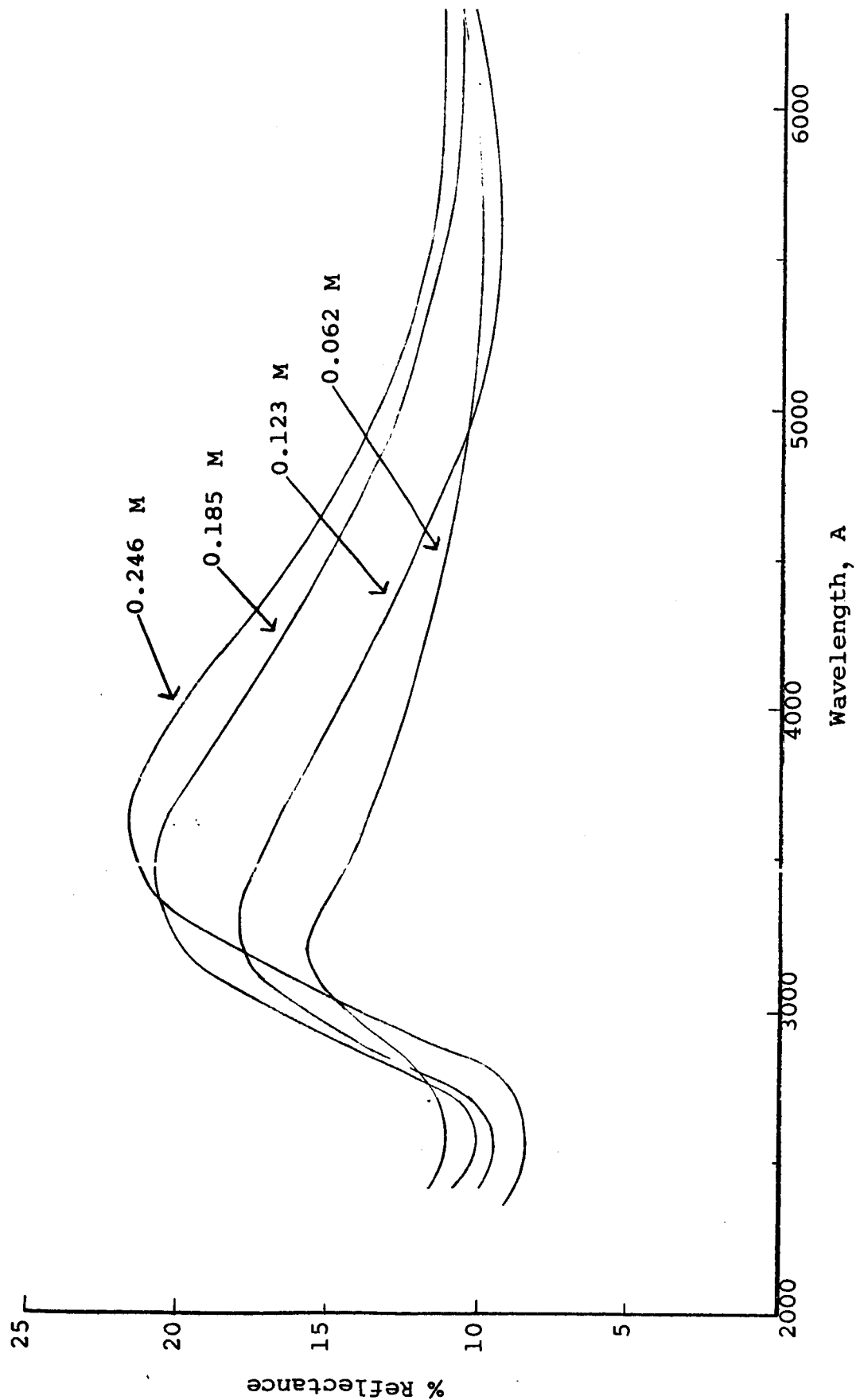


Figure 14

REFLECTANCE OF COATINGS OF SILVER CHLORIDE SUSPENSIONS
IN GELATIN AT VARIOUS CONCENTRATIONS (RELATIVE TO MgCO_3)

B. Angular Scattering of Light By Silver Chloride Films

Attempts were made to determine the angular distribution of scattered light by the monodisperse silver chloride films described in our last quarterly report. The relative concentrations of silver chloride in gelatin were 0.06, 0.123, 0.185, and 0.246 M, and the films were spread on a quartz substrate (see Section IVA). The Brice-Phoenix light-scattering photometer with the schematic film orientation shown in Figure 15 was used for this study.

For the particular experimental arrangement employed, the intensity of scattered light per unit area of film, $I(\theta)$, at an angle, θ , is given by

$$I(\theta) = \frac{F(\theta)}{A \sin \theta}$$

where $I(\theta)$ is intensity/unit area

θ is the angle of observation measured from the plane of the film

A is the area covered by the illuminating beam

$F(\theta)$ is total light flux at angle θ .

The measurements were obtained by using green (0.546- μ) and blue (0.436- μ) mercury lines as sources of unpolarized monochromatic light. One measurement was also obtained with total mercury radiation (unpolarized) and without filters; in this case approximately 90% of the energy was in the ultraviolet mercury line (0.254 μ).

The results are summarized in Figures 16, 17, and 18 and show the intensity/area (arbitrary relative intensity units) as a function of the angle of observation. The notation of

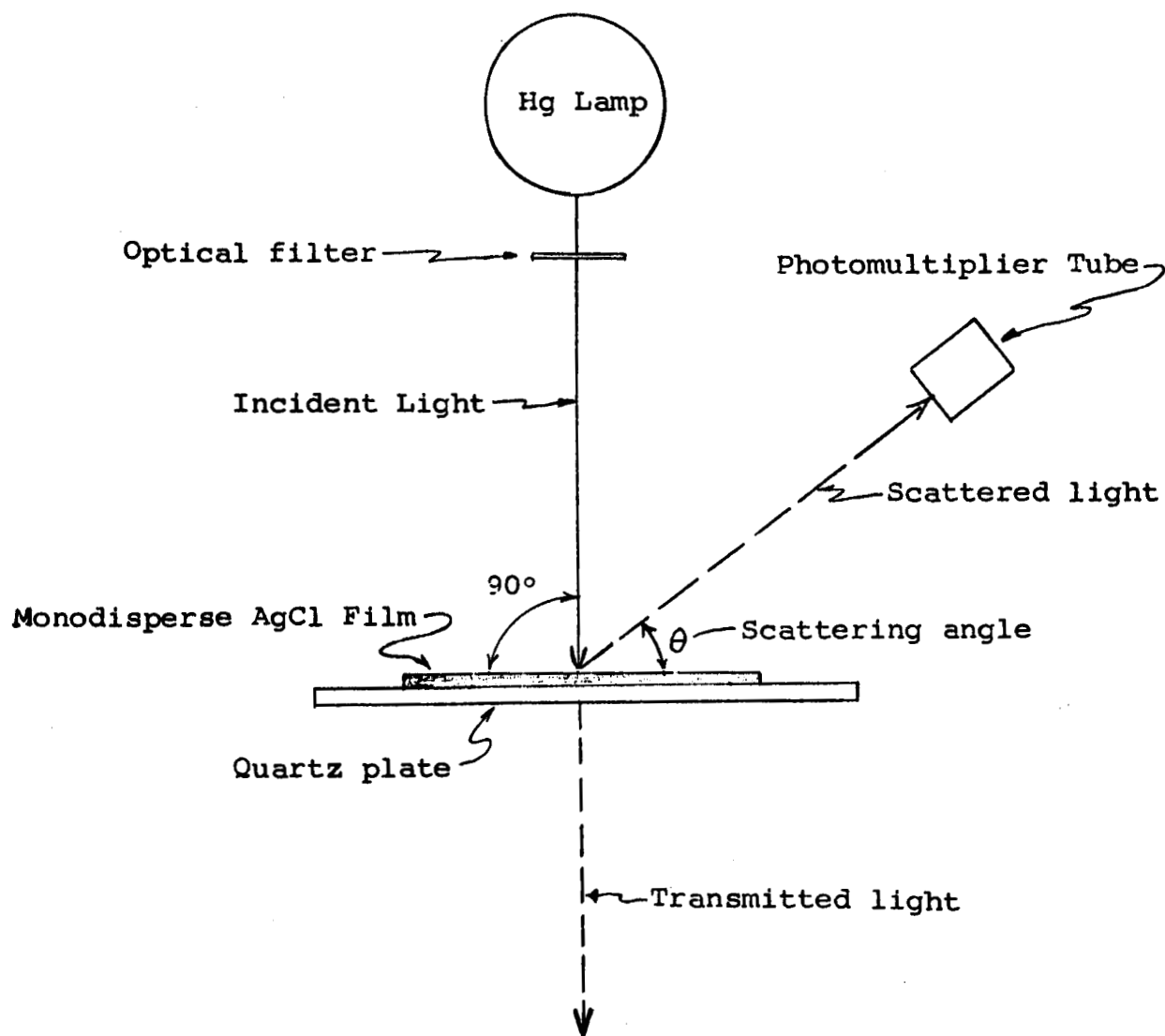


Figure 15

BRICE-PHOENIX LIGHT-SCATTERING PHOTOMETER

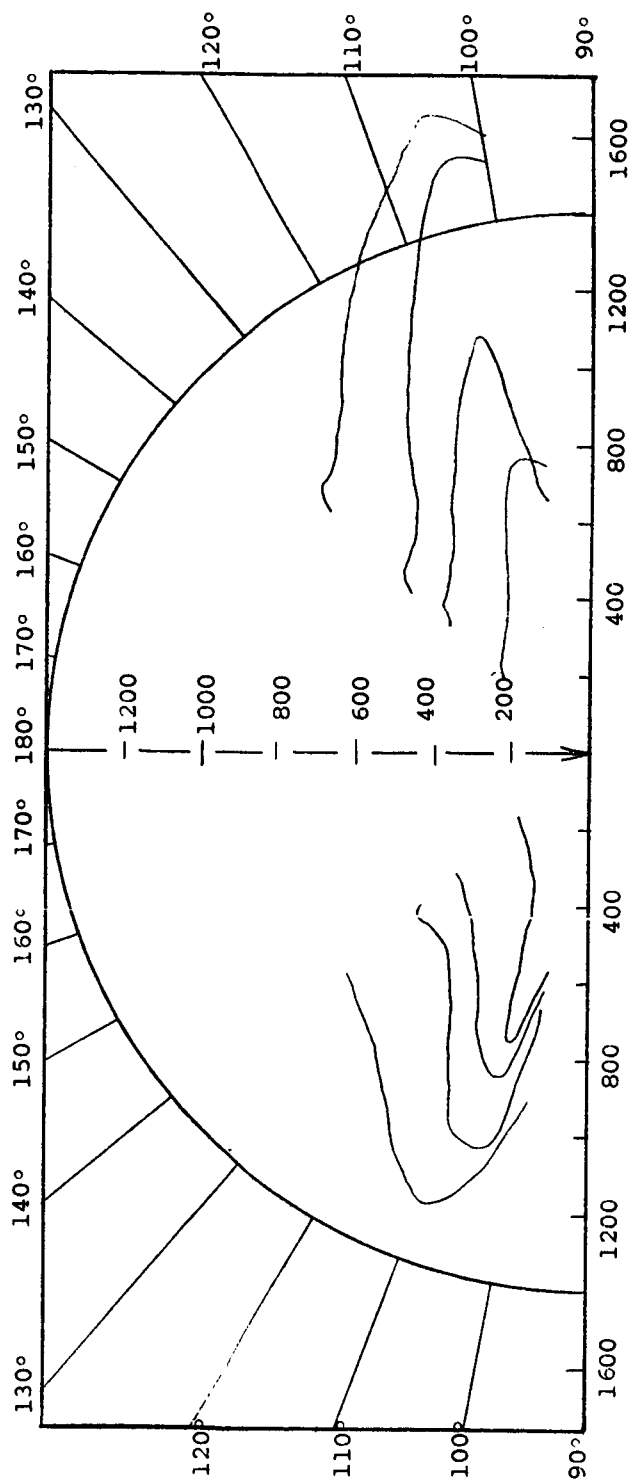


Figure 16
INTENSITY/UNIT AREA OF BLUE MERCURY LINE VERSUS ANGLE OF OBSERVATION

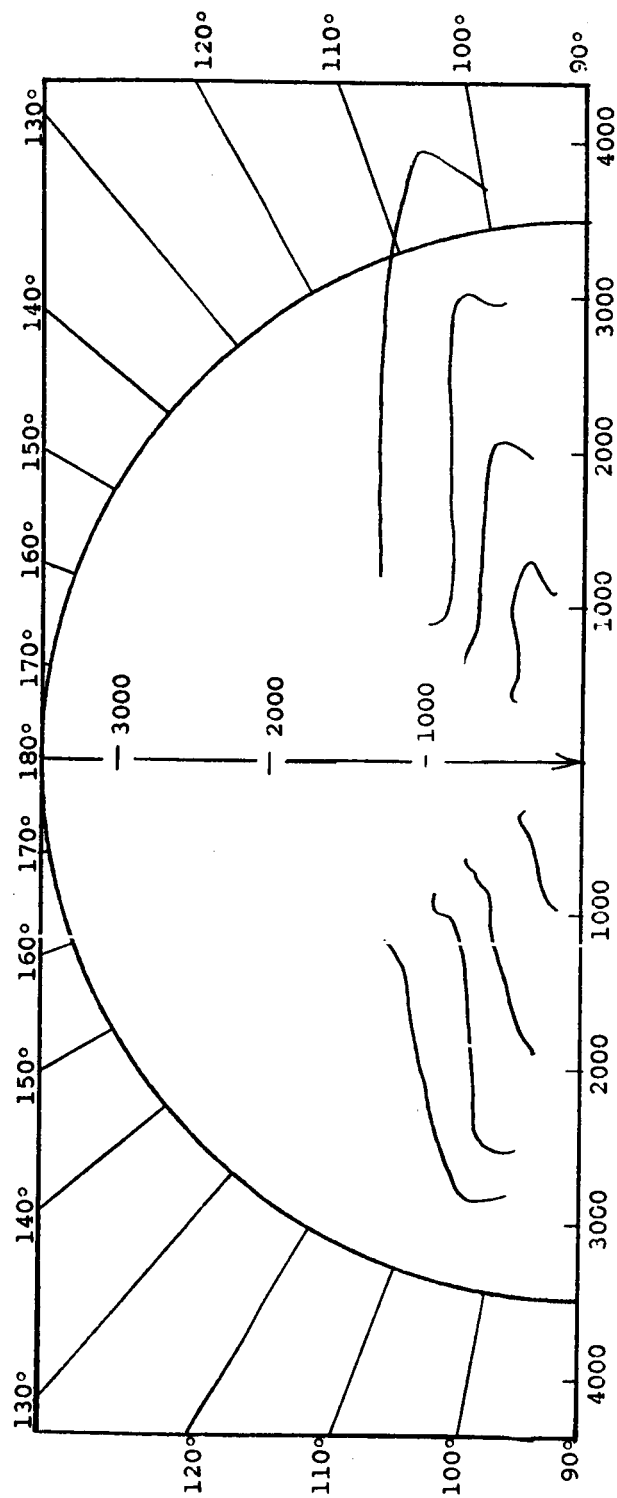


Figure 17
INTENSITY/UNIT AREA OF GREEN MERCURY LINE VERSUS ANGLE OF OBSERVATION

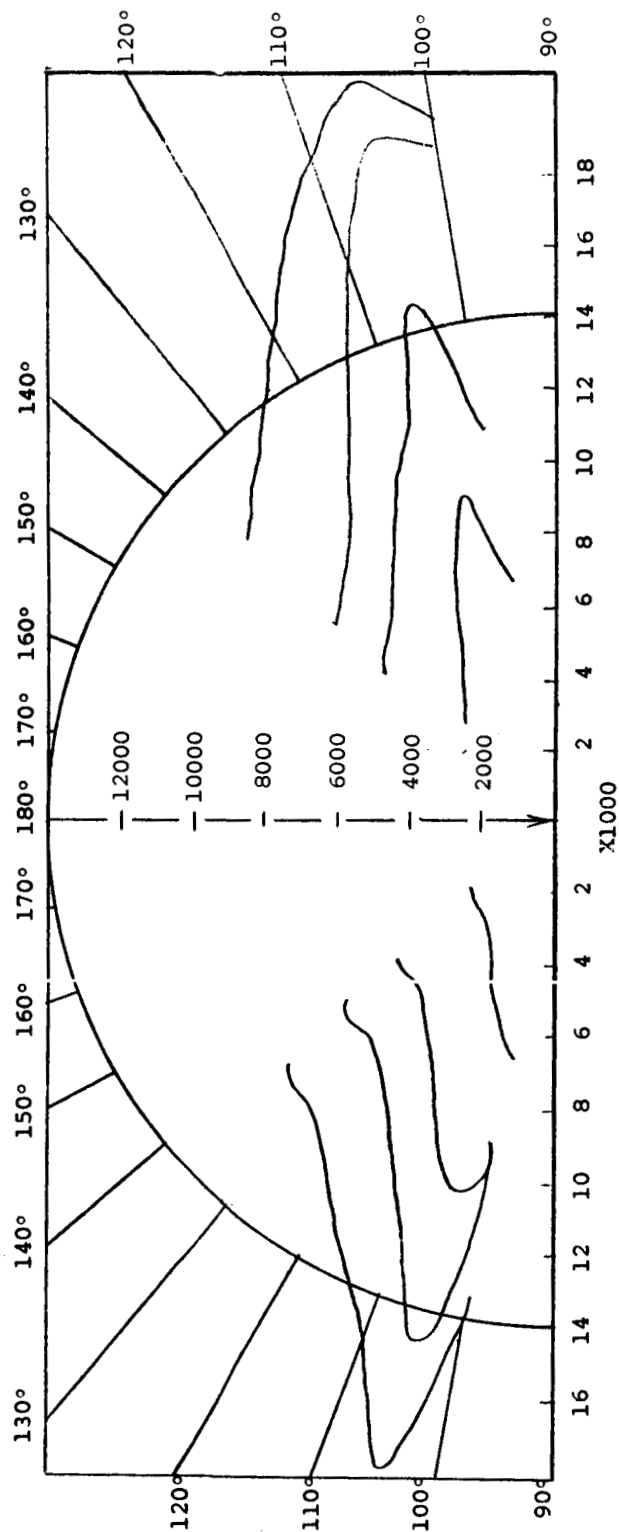


Figure 18
INTENSITY/UNIT AREA OF TOTAL MERCURY RADIATION VERSUS ANGLE OF OBSERVATION

angles corresponds to the one used with the Brice-Phoenix light scattering photometer.

It has been shown previously that the intensity of radially scattered light is dependent on the size parameter α , where $\alpha = 2\pi r/\lambda$.⁸ The angular distribution of back-scattered intensity for two particle sizes is given in Figure 19. Films prepared from batches 8 and 12 (described previously) were used, and the blue mercury line at 0.436μ was used as the illuminating beam. The estimated values of α were ≈ 1.5 for batch 8 and ≈ 7.3 for batch 12. Examination of Figure 19 reveals significant changes in total intensity and radial distribution of back-scattered light with varying particle size. Comparison with the theoretically predicted distribution gives at least a qualitative agreement.⁹

C. Reflectance and Transmittance Measurements of Monodisperse Silver Chloride Films of Various Particle Sizes

The transmittance and reflectance measurements have recently been extended to films of silver chloride crystals of various particle sizes. Two batches of silver chloride crystals with significantly different average particle sizes were

⁸Quarterly Report IITRI-C6018-3, pp. 5 and 8.

⁹Ibid, Figure 2, p. 10.

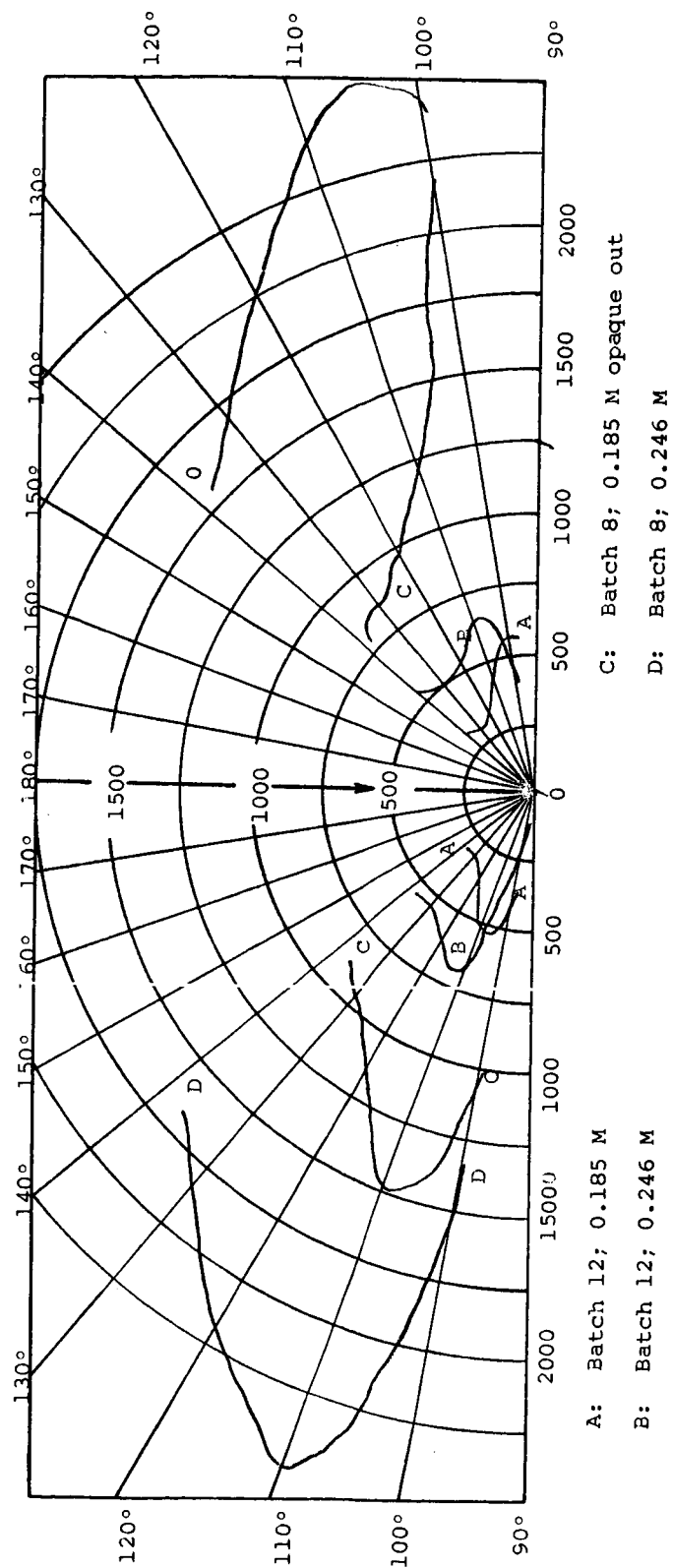


Figure 19

RADIAL DISTRIBUTION OF INTENSITY OF BACK-SCATTERED LIGHT
 FOR VARIOUS PARTICLE SIZES

chosen for initial trials. It is estimated that the average particle diameter of the two batches varied by a factor of five. Batch 8 had an estimated length of the cube edge of less than 0.2μ and batch 12 of approximately 1.5μ .

A series of films of various concentrations were made in each case. The spectral reflectance and transmittance curves are given in Figures 20 and 21.

Examination of Figure 20 reveals that the larger particles (batch 12) gave considerably lower reflectance at any given concentration, with a slight, uniform increase toward the shorter wavelengths. The smaller particles (batch 8) gave a reflectance maximum at approximately 0.38μ , which was also noted in our earlier studies. It is believed that the scattering effects of the larger particles were too small to be detected. This observation seems to be confirmed by the spectral transmittance curves of Figure 21. In our earlier studies with various concentrations, a transmittance minimum was noted at 0.28μ . This minimum seems to be completely absent with films of larger particles.

It was suggested that the transmittance minimum at 0.28μ could be due to the lattice vibrations of metallic silver present in silver chloride crystals. This postulate was tested by exposing the films to an intense ultraviolet light until noticeable darkening occurred, indicating an increase in the concentration of free silver. No significant change in the absorption minimum at 0.28μ was observed in the

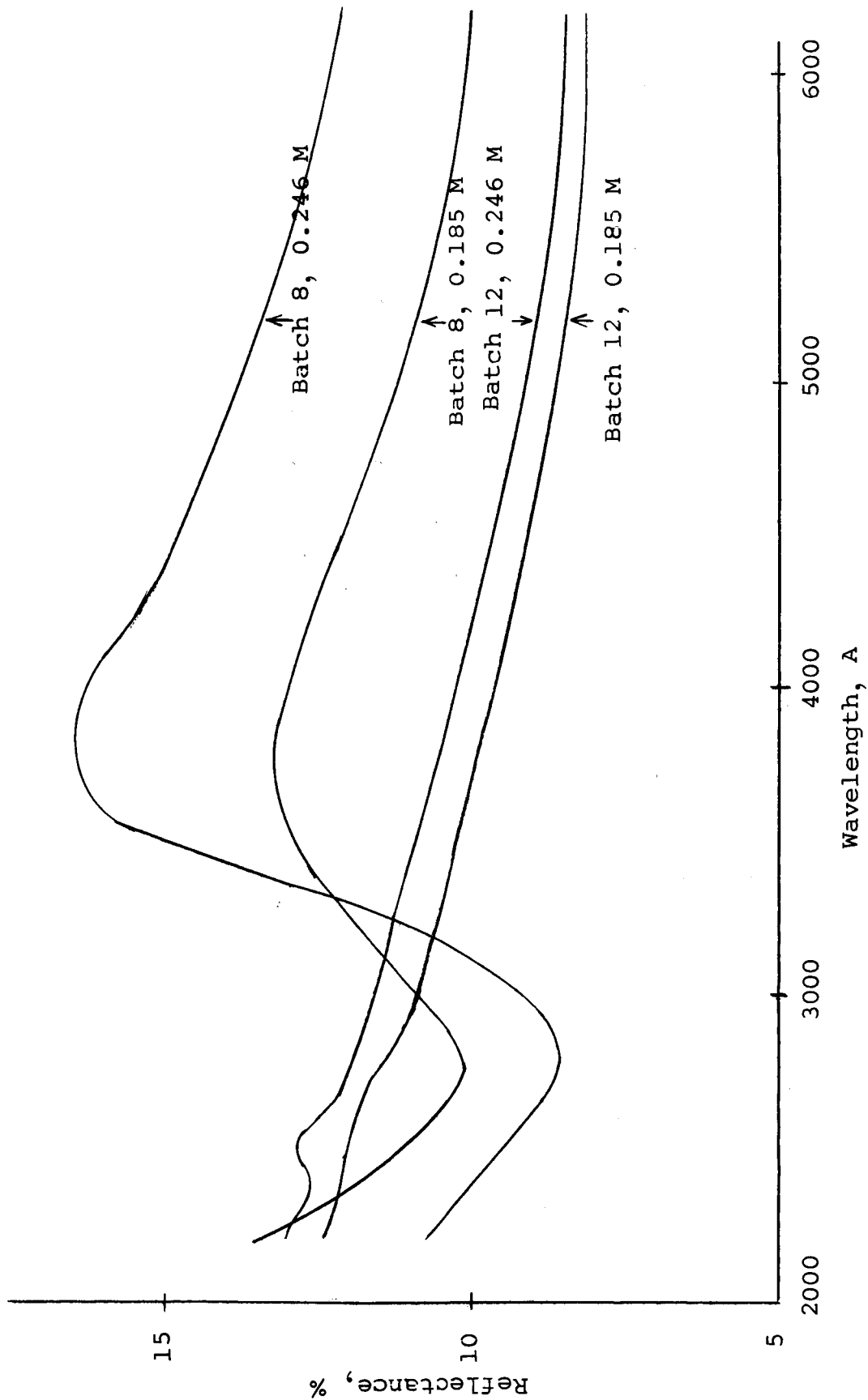


Figure 20
REFLECTANCE OF SILVER CHLORIDE COATINGS
OF VARIOUS PARTICLE SIZES AND CONCENTRATIONS

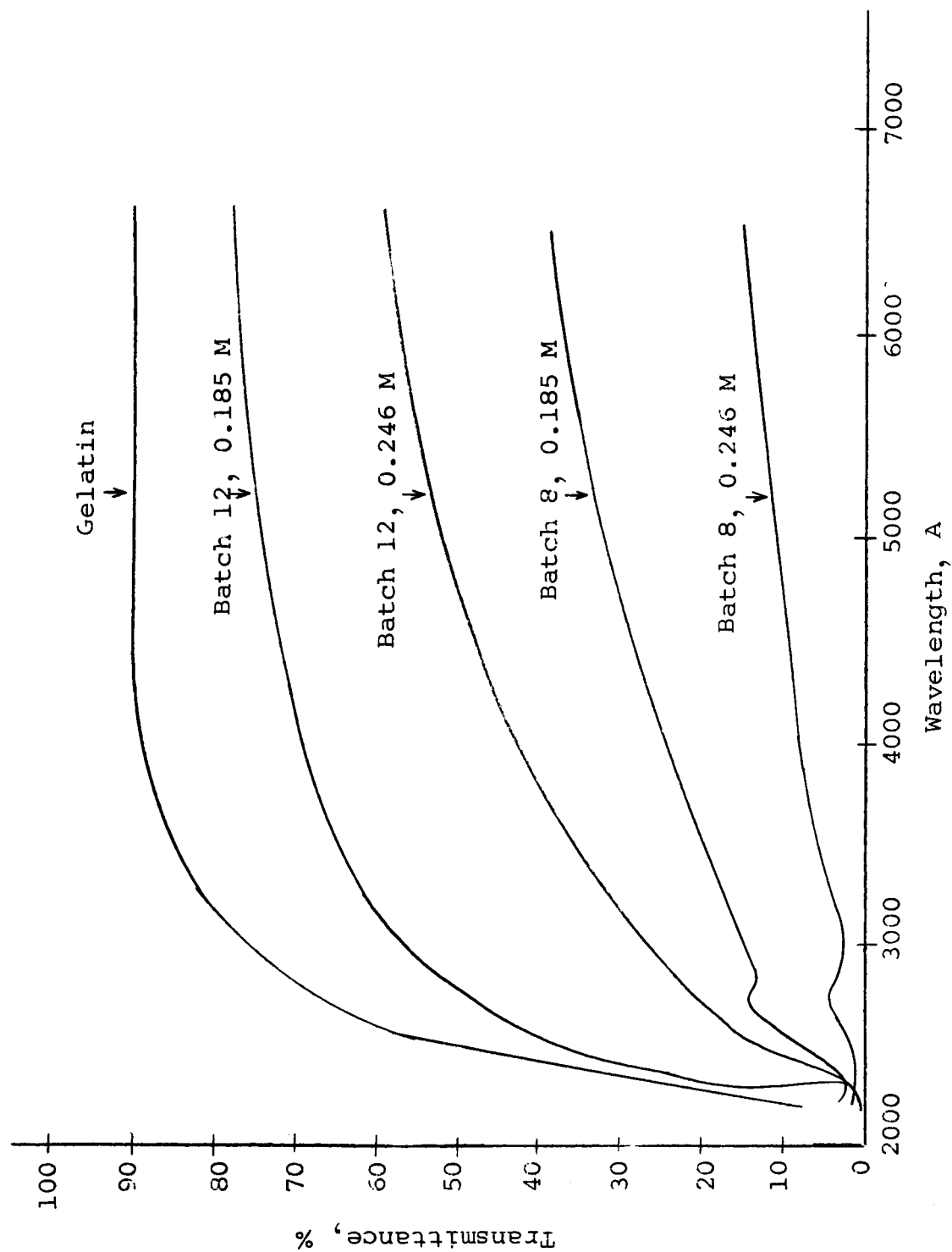


Figure 21

TRANSMITTANCE OF SILVER CHLORIDE COATINGS
OF VARIOUS PARTICLE SIZES AND CONCENTRATIONS

darkened films; this suggested that the transmittance minimum at 0.28μ is probably due to the light-scattering effects of silver chloride crystals.

Another observation from Figure 21 is that the transmittance of films containing larger particles increases considerably at all wavelengths for any given concentration.

V. FUTURE WORK

In the next phase of the theoretical analysis, scattering by multiple arrays of particles will be considered. In addition, the light-scattering properties of materials will be examined in relation to the problems of emissivity and reflectance control.

A procedure has been worked out to normalize all radial distribution measurements so that quantitative comparisons will be possible for various particle sizes and also for measurements at different wavelengths. In addition, the measurements will be extended to include front scatter and lower angles in back scatter and will include work with plane-polarized light as well as nonpolarized light.

DISTRIBUTION LIST

This report is being distributed as follows:

<u>Copy No.</u>	<u>Recipient</u>
1-25 + repro- ducible	National Aeronautics and Space Administration Office of Grants and Research Contracts Washington, D. C.
26	National Aeronautics and Space Administration Office of Advanced Research and Technology Washington 25, D. C. ATTN: Mr. J. J. Gangler
27	George C. Marshall Space Flight Center Huntsville, Alabama ATTN: Mr. D. W. Gates (M-RP-T)
28	Mr. Conrad Mook Code RV National Aeronautics and Space Administration Washington, D.C.
29	Mr. Omar K. Salmassy Code MSA National Aeronautics and Space Administration Washington, D. C.
30	Mr. Sam Katzoff National Aeronautics and Space Administration Langley Research Center Langley Field, Virginia
31	Mr. Joseph C. Richmond National Bureau of Standards Washington, D. C.
32	Mr. James Diedrich Mail Stop 7-1 Lewis Research Center Cleveland, Ohio
33	Jet Propulsion Laboratory 4800 Oak Grove Drive Pasadena, California ATTN: Mr. William F. Carroll Materials and Methods

DISTRIBUTION LIST (cont.)

<u>Copy No.</u>	<u>Recipient</u>
34	IIT Research Institute Division C Files
35	IIT Research Institute Editors, J. J. Brophy, J. I. Bregman, Main Files
36	IIT Research Institute K. W. Miller, Report Library
37	IIT Research Institute D. Levinson, Division B
38	IIT Research Institute E. H. Tompkins, Division C
39	IIT Research Institute G. A. Zerlaut, Division C
40	IIT Research Institute S. Katz, Division C
41	IIT Research Institute J. Allen, Division C
42-44	IIT Research Institute J. Stockham, Division C
45	IIT Research Institute Y. Harada, H. Rechter, Division B